Journal of Geophysical Research: Biogeosciences

RESEARCH ARTICLE
10.1029/2018JG004659

Special Section:
The Arctic: An AGU Joint Special Collection

Seasonal and Geographic Variation in Dissolved Carbon Biogeochemistry of Rivers Draining to the Canadian Arctic Ocean and Hudson Bay

Joanna Y. S. Li Yung Lung[1†], Suzanne E. Tank[1†], Christopher Spence[2], Daqing Yang[3], Barrie Bonsal[2], James W. McClelland[4], and Robert M. Holmes[5]

[1]Department of Biological Sciences, University of Alberta, Edmonton, Alberta, Canada, [2]Watershed Hydrology and Ecology Research Division, Environment and Climate Change, Saskatoon, Saskatchewan, Canada, [3]Water and Climate Impacts Research Centre, Environment and Climate Change, Victoria, British Columbia, Canada, [4]Marine Science Institute, University of Texas at Austin, Port Aransas, TX, USA, [5]Woods Hole Research Center, Falmouth, MA, USA

†These authors contributed equally to the manuscript.

Key Points:
- The concentration and flux of organic and inorganic carbon vary substantially across Canadian Arctic rivers but track latitude and physiographic region
- Alkalinity in this region is largely derived from carbonate weathering, with sulfide oxidation potentially an important contributor to the weathering flux
- Geographic and temporal data gaps hamper our ability to definitively quantify riverine chemistry through large swaths of northern Canada

Supporting Information:
- Supporting Information S1
- Data Set S1

Correspondence to:
S. E. Tank,
suzanne.tank@ualberta.ca

Citation:
Li Yung Lung, J. Y. S., Tank, S. E., Spence, C., Yang, D., Bonsal, B., McClelland, J. W., & Holmes, R. M. (2018). Seasonal and geographic variation in dissolved carbon biogeochemistry of rivers draining to the Canadian Arctic Ocean and Hudson Bay. *Journal of Geophysical Research: Biogeosciences*, *123*, 3371–3386. https://doi.org/10.1029/2018JG004659

Received 21 JUN 2018
Accepted 10 SEP 2018
Accepted article online 17 SEP 2018
Published online 24 OCT 2018

Abstract The chemical composition of river water can be used to diagnose change on land, while playing a determining role in the ecology and biogeochemistry of riverine-influenced ocean waters. Despite this, little is known about the seasonal and geographic variability of riverine chemistry throughout much of the Canadian north. Here we assess the chemical composition of a broad suite of rivers draining to the Canadian Arctic Ocean and Hudson Bay using previously unpublished government data. We focus on inorganic and organic carbon (alkalinity and dissolved organic carbon), using paired chemistry and discharge measurements to assess constituent flux. Concentrations and area-normalized yields vary substantially across the northern Canadian landscape, with dissolved organic carbon typically highest in rivers draining the Hudson Bay Lowland, alkalinity highest in rivers draining Cordillera and Plains terrains, and the ratio of organic to inorganic species highest in rivers draining the Canadian Shield. Yields of major weathering ions show that carbonate weathering—a notable proportion of which may be driven by sulfide oxidation—dominates inorganic carbon delivery from the rivers we assess. Despite the reasonably diverse coverage of the data set, we find that clear gaps exist, including a lack of data through to the present day for many rivers, and a dearth of measurements from the Arctic Archipelago and eastern shores of Hudson Bay. We therefore use a modeling approach to extrapolate fluxes to the full Canadian Arctic drainage basin. Region-specific differences between our results and previous models reinforce the need for targeted river water chemistry measures throughout the Canadian Arctic domain.

1. Introduction

The flow of rivers from land to ocean exerts an underlying control on the physical, biogeochemical, and ecological functioning of nearshore regions. This is particularly true in the Arctic, where an ocean basin encompassing ~1% of the world's ocean surface volume receives ~10% of its riverine runoff (McClelland et al., 2012). As a result, freshwater inputs play a key role in shaping the rate, distribution, and seasonality of processes such as primary production (Tremblay et al., 2015), ocean acidification (Mathis et al., 2011; Tank et al., 2012), and microbial metabolism (Ortega-Retuerta et al., 2012) in the nearshore Arctic. Despite this, our understanding of the chemical composition of river water throughout much of the Arctic drainage basin is relatively poor, particularly outside of major rivers (McClelland et al., 2015).

There has been a concerted effort to quantify the chemistry of the six largest rivers that flow to the Arctic Ocean (Holmes et al., 2013). However, despite the important progress that has been made to quantify the biogeochemistry of these large systems, these "great" rivers typically have watersheds that extend well into permafrost-free regions (Holmes et al., 2013), and hydrologic regimes characteristic of large, diverse drainage basins (e.g., White et al., 2007; Yang et al., 2007, 2015). As a result, these large systems are unlikely to be representative of the distributed array of smaller watersheds that comprise a significant proportion of the Arctic basin. Measurements characterizing the biogeochemistry of smaller rivers in Alaska (Townsend-Small et al., 2011), Siberia (Johnston et al., 2018), around Hudson Bay (Godin et al., 2017), and in the Canadian Arctic Archipelago (Alkire et al., 2017) have provided well-defined estimates of water chemistry, but over relatively constrained spatial scales, or—because of

logistical constraints—based on a relatively small number of samples. In Canada in particular, we know little about the 75% of the Arctic-flowing drainage that lies outside of the well-characterized Mackenzie system (see also Alkire et al., 2017 and Godin et al., 2017, for recent progress). This lack of knowledge exists despite evidence of increasing fluxes of dissolved carbon and ions from several Canadian Arctic locations, which appear to be driven by thawing permafrost and other factors related to climate change (Kokelj et al., 2013; Spence et al., 2015; Tank et al., 2016).

In addition to its importance for regulating nearshore ocean processes, the chemical composition of river water can provide important insights into the state, and rate of change, of processes occurring on land. From a carbon cycle perspective, both dissolved organic and dissolved inorganic carbon (DOC and DIC) at the mouths of large rivers can help elucidate fixation (from CO_2) and mineralization (to CO_2) of carbon species across the aquatic continuum. For example, although DOC measured at river mouths represents just a fraction of the organic carbon that enters the aquatic continuum (e.g., Drake et al., 2017; Tank et al., 2018), we do know that much of this reduced carbon will be mineralized within the Arctic Ocean basin (e.g., Alling et al., 2010). In contrast, the non-CO_2 component of DIC is largely derived from chemical weathering, which acts as a key geological CO_2 sink when driven by carbonic acid (Berner & Berner, 2012). Thus, understanding the balance between organic and inorganic carbon at the mouths of major rivers, and the provenance of the various species that comprise the dissolved carbon pool, can provide important insights into the functioning of the carbon cycle over broad spatial scales.

As a result of the tight connection between fluvial systems and the landscapes that surround them, between-catchment differences in landscape attributes drive geographic variation in the chemical composition of river water. In Arctic regions, for example, DOC concentration and flux have been shown to be regulated by within-catchment permafrost extent, soil organic carbon content and/or catchment slope, and runoff (Connolly et al., 2018; Harms et al., 2016; Tank et al., 2012). Similarly, the concentration and flux of DIC and major ions is fundamentally driven by catchment lithology (Moosdorf et al., 2011) but also affected by factors such as permafrost and runoff (Tank, Raymond, et al., 2012). Within the Canadian Arctic drainage basin, runoff patterns (Déry et al., 2009; Spence & Burke, 2008), soils (Soil Landscapes of Canada Working Group, 2010), and lithology (Wheeler et al., 1996) show striking regional variation. This variation is exemplified by the array of physiographic regions found across northern Canada, which range from till-dominated Plains in the west to Precambrian Shield and peatland-rich lowlands in the east (Figure 1). To date, the chemistry of many of the riverine systems draining these diverse landscapes has been poorly documented.

The purpose of this study was to characterize the chemical composition of rivers within the Canadian Arctic drainage basin and to assess the status of data availability for this region. To accomplish this task, we explored previously unpublished data that have been collected through monitoring efforts by Environment and Climate Change Canada and associated Provincial and Territorial government agencies. We use these data to calculate the flux of carbon and major ions from individual rivers, explore spatial and seasonal variation in concentration and flux, understand the carbon cycle implications of the chemical composition of export from these rivers, and extrapolate the flux of organic and inorganic carbon to the broader Canadian Arctic Ocean drainage. The result is the broadest assessment to date of the chemistry of Canadian rivers flowing to the Arctic Ocean, and a preliminary assessment of the monitoring systems meant to document the current state and potential change in freshwater flux to the Canada's nearshore Arctic Ocean.

2. Study Region

The Canadian Arctic drainage basin encompasses a series of five major physiographic regions (Figure 1). In the far west, the Mountain Cordillera extends through the Richardson Mountains, Mackenzie Mountains, and northern Rocky Mountains, with a geology largely comprised of strongly folded sedimentary strata with some igneous intrusions (Clayton et al., 1977; Wheeler et al., 1996). Soils in this region typically have defined organic and well-developed mineral horizons (in the Canadian classification system, generally turbic cryosols where permafrost is present, and podsols, brunisols, and luvisols elsewhere; Soil Landscapes of Canada Working Group, 2010). East of the Cordillera, the geology of the Interior Plains consists of sedimentary limestones, sandstones, and shales, which overlie the western rim of the Precambrian Shield. These sedimentary deposits are in turn overlain by glacial tills that vary in thickness but can reach hundreds of meters depth

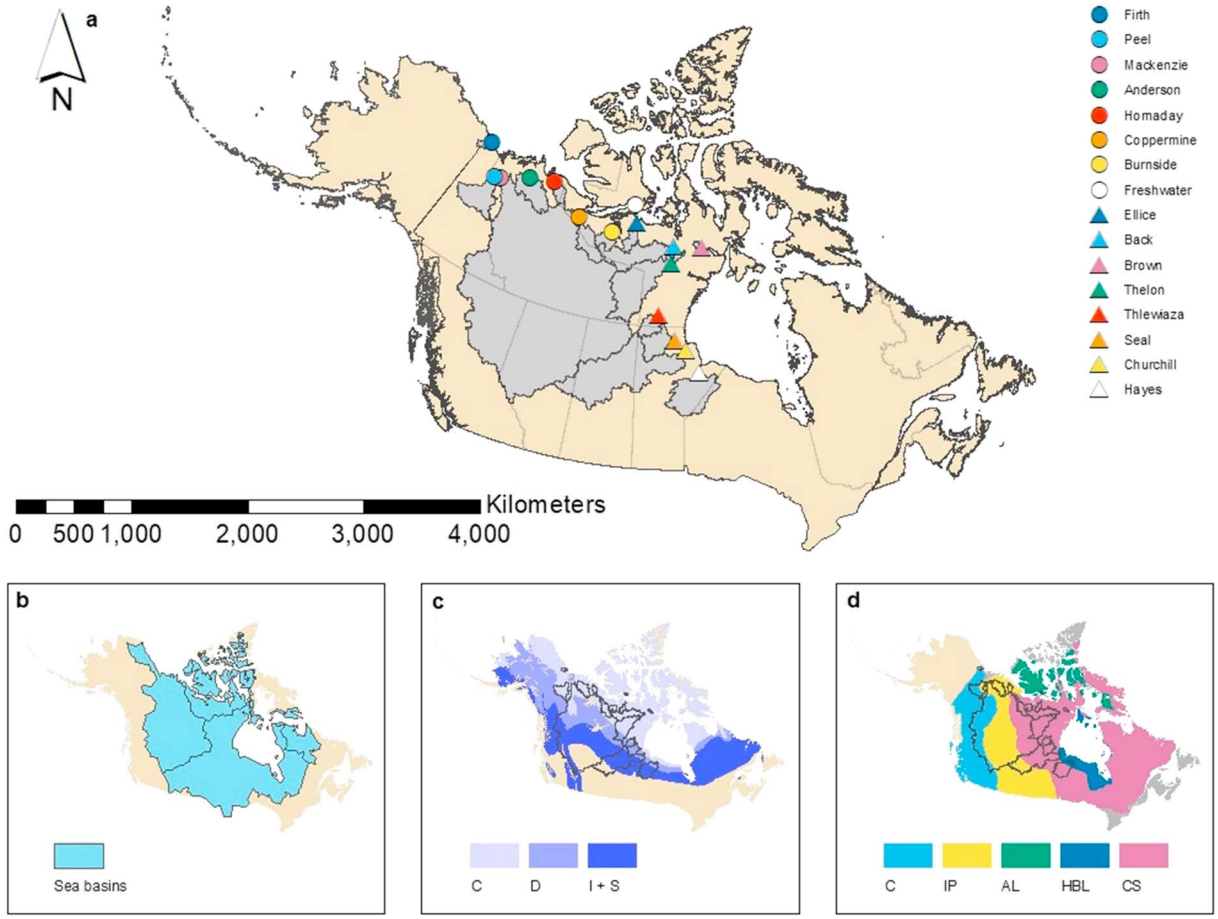

Figure 1. (a) A map of the 16 study watersheds, showing the discharge station and upstream watershed. (b) The four sea basins used to extrapolate DOC and alkalinity flux: from west to east, the Beaufort Sea, Arctic Archipelago, Hudson Bay, and Hudson Strait sea basins presented in Lammers et al. (2001). (c) Distribution of continuous (C), discontinuous (D), and isolated + sporadic (I + S) permafrost across the study domain. (d) Distribution of physiographic regions across the study domain, including the Cordillera (C), Interior Plains (IP), Arctic Lowlands (AL), Hudson Bay Lowland (HBL), and Canadian Shield (CS). In panel (a), catchments are labeled from west to east, following the coast.

(Fenton et al., 1994). While well-developed mineral soils (turbic cryosols, luvisols, and brunisols) are also characteristic of this region (Soil Landscapes of Canada Working Group, 2010), peatland complexes composed of flat bogs, channel fens, and peat plateaus are common throughout permafrost-affected terrains (Quinton et al., 2003). Immediately south and west of James and Hudson Bay, the Hudson Bay Lowland is a vast wetland/peatland complex underlain by flat deposits of Paleozoic limestones and dolomites (Clayton et al., 1977; Wheeler et al., 1996). The extensive peatlands in this region have been forming for the past 5,000 years and can reach 3- to 4-m depth (Martini, 1989).

In contrast to the sedimentary deposits of the west and lowland regions, the Canadian Shield is comprised of poorly weatherable intrusive igneous and metamorphic rocks of Precambrian origin, with some imbedded volcanic and sedimentary assemblages (Clayton et al., 1977; Wheeler et al., 1996). Although glacial action did deposit thin, sandy tills in landscape depressions throughout the Shield region, it also caused extensive areas to be fully denuded of soil material. Overlying soils are influenced by this geologic and glacial history and tend to be shallow, with the exception of an organic-rich region adjacent to the north-west edge of the Hudson Bay Lowland. Soils of the Arctic Lowland region are also typically shallow and entirely composed of mineral (static and turbic) cryosols (Soil Landscapes of Canada Working Group, 2010). However, unlike the Canadian Shield, the underlying geology of the Arctic Lowlands is largely sedimentary (Wheeler et al., 1996). Permafrost throughout the Canadian Arctic drainage basin ranges from continuous in the north, to fully absent in the south (Figure 1), and this variation is captured by the various river basins that drain north to the Arctic Ocean and Hudson Bay.

Table 1
Site Characteristics for the 16 Watersheds Used for This Work

River	Physiographic region	Latitude	Longitude	Basin area (km^2)	Runoff (mm/year)	C (%)	D (%)	S (%)	I (%)	SOCC (kg/m^2)	SC (%)	SM (%)	SS (%)	SU (%)	VB (%)
Firth	Cordillera	69.33	−139.57	5,714	164.2	100	0	0	0	12.2	33.6	21.8	37.2	6.9	0.0
Peel	Plains-Cordillera	67.26	−134.89	70,680	301.0	85.1	14.9	0	0	14.8	19.2	42.8	29.0	8.4	0.2
Mackenzie	Plains-Cordillera-Shield	67.46	−133.75	1,673,883	166.2	12.4	30.6	29.4	11.2	24.9	12.2	24.2	41.1	0.7	0.5
Anderson	Plains	68.63	−128.42	56,241	75.1	100	0	0	0	50.4	36.5	4.3	59.2	0	0
Hornaday	Plains	69.18	−123.25	14,033	181.6	100	0	0	0	27.8	36.5	55.4	1.3	0	0
Coppermine	Shield	67.23	−115.89	47,405	179.4	99.7	0.3	0	0	17.1	0	42.6	0	0	5.0
Burnside	Shield	66.73	−108.81	19,567	229.1	100	0	0	0	19.9	0	39.3	0	0	0.1
Freshwater	Arctic Lowlands	69.13	−104.99	1,569	232.9	100	0	0	0	46.0	100	0	0	0	0
Ellice	Shield	67.71	−104.14	17,096	349.2	100	0	0	0	14.0	0	3.0	0	0	0
Back	Shield	66.09	−96.51	96,965	146.2	100	0	0	0	11.5	0	17.1	5.4	0	0.2
Brown	Shield	65.93	−91.07	4,695	361.1	100	0	0	0	27.7	0	0	0	0	1.3
Thelon	Shield	64.78	−97.05	152,417	184.1	80.0	20.0	0	0	12.2	0.0	17.9	21.8	0	0.2
Thlewiaza	Shield	60.79	98.78	27,434	281.5	33.6	66.4	0	0	5.9	0	11.4	0	0	0.4
Seal	Wetland-rich shield	58.89	−96.28	48,157	236.0	10.4	77.2	12.3	0	11.0	0	0.1	0	0	0.1
Churchill	HBL-Shield-Plains	58.12	−94.62	289,409	24.3	0.0	9.5	57.8	7.7	23.0	0.1	9.4	32.4	0	1.0
Hayes	HBL-Shield	56.42	−92.81	102,741	166.7	0.5	18.7	61.5	19.0	32.4	11.0	6.4	1.8	0	6.8

Note. Coordinates are provided for the location of the gauging station; basin area is calculated as area upstream of the station. For catchments that span more than one physiographic region, regions are listed in descending order of importance. Runoff data are for the partial record as provided in Table S2. C, D, S, and I indicate percent continuous, discontinuous, sporadic, and isolated permafrost in the delineated basin (Brown et al., 1998); SOCC indicates mean soil organic carbon content in kilogram per square meters (Tarnocai et al., 2007). SC, SM, SS, SU, and VB indicate percent carbonate sedimentary rocks, mixed sedimentary rocks, siliciclastic sedimentary rocks, unconsolidated sediments, and basic volcanic rocks respectively (Dürr et al., 2005; Jansen et al., 2010). HBL refers to Hudson Bay Lowland.

3. Methods

3.1. Data Acquisition and Initial Data Assessment

Daily water discharge data were obtained directly from the Water Survey of Canada (https://wateroffice.ec.gc.ca). We targeted gauging stations draining directly into the Arctic Ocean or Hudson Bay, using the most downstream station when multiple stations were present within the same river system. Water chemistry data from candidate stations were obtained following requests to Environment and Climate Change Canada and various provincial monitoring agencies. This initial scoping exercise identified 16 stations with matching water chemistry and discharge data (Figure 1 and Table 1), and a series of stations with discharge, but no, or sparse, water quality information (Table S1).

We consider alkalinity, DOC, Ca, Mg, Na, and SO_4 in our analyses. We chose these parameters because they are widely available across river systems and because they broadly describe organic and inorganic (i.e., weathering) carbon processes. Nutrient data were also acquired for our initial analyses but were often below detection, making further assessment difficult. A quality control check on individual water chemistry data points was conducted by constructing concentration discharge (C-Q) plots and discarding data that lay well outside of the concentration: discharge relationship. This step eliminated 107 of the 6,794 concentration data points that we considered. Where multiple water chemistry measurements existed on a single day, a single mean daily value was calculated. Short gaps in the discharge record (either $<$22 days or late in the fall season) were filled by linear interpolation, following visual inspection to confirm that flow was changing in a consistent manner, based on the recorded conditions surrounding the gap and comparison with other years. When consistent change could not be confirmed, the year was excluded from calculations of annual means. Larger winter-time gaps were assumed to represent zero flow when the data gap was surrounded by discharge measurements that declined to zero during the preceding fall, and resumed from zero (or, near zero) during the following spring. Of 264 years of coupled chemistry-discharge data, 11 nonwinter gaps were filled, and 23 years were excluded from the calculations of annual means that we present. The majority of excluded years were on the Churchill and Hayes Rivers.

3.2. Calculation of Constituent Flux

Constituent flux estimates were calculated using LoadRunner (Booth et al., 2007), which automates the Fortran-based U.S. Geological Survey Load Estimator program, LOADEST (Runkel et al., 2004). LOADEST

uses a time series of paired streamflow and constituent concentration data to construct a calibration regression, which is then applied to a daily discharge record to obtain daily constituent fluxes (load; mass/day), where load is the product of constituent concentration (mass/volume) and discharge (volume/day). The program uses a series of models, which are nested within the following:

$$\ln\widehat{L} = a_0 + a_1 \ln Q + a_2 \ln Q^2 + a_3 \sin(2\,\pi \mathrm{dtime}) + a_4 \cos(2\,\pi \mathrm{dtime}) + a_5 \mathrm{dtime} + a_6 \mathrm{dtime}^2, \quad (1)$$

where $\ln\widehat{L}$ is the natural log of the load estimate, lnQ = ln (streamflow)—center of ln (streamflow), and dtime = decimal time—center of decimal time. We used the Akaike information criterion to select the model of best fit from among the nested series of potential models, following common practice when there is no a priori reason for model preference (Burnham & Anderson, 2002). The Adjusted Maximum Likelihood Estimator (AMLE) was used to fit the calibration equation, as is best practice for LOADEST output models where the calibration model errors are normally distributed, and no censored data (i.e., concentrations below the laboratory detection limit) are present (Runkel et al., 2004).

Models for the Churchill and Seal Rivers were run using both full and partial time series of the data. On the Churchill River, the diversion that was implemented in 1976 caused a significant change in streamflow, with a transition period between the unregulated and regulated flow regime that persisted until 1980 (Crawford, 2015). As a result, we ran models for the Churchill River that included all available data (1973–1996) and data only from the posttransition period (1980–1996). On the Seal River, the full 1972–2001 data set has a 13-year data gap in water chemistry between 1978 and 1991, and we therefore modeled flux using data from the full period of record and data for only the second measurement period (1991–2001). In all cases, LOADEST model fits were assessed by inspecting plots of estimated and calculated loads and the residuals of the model output.

Modeled daily flux values were used to calculate annual constituent loads (as mass/year) for all years where a full yearly length of discharge data was present (see section 3.1). On the Hornaday and Firth Rivers, discharge measurements begin in the spring, a few days after flow had commenced, and end in the fall, before the cessation of flow. As a result, the outputs for these rivers represent partial annual fluxes, although on the Hornaday River, spring and fall gaps were short enough that early, full-season discharge records could be used to estimate missing early and late season discharge, which accounted for approximately 1% of the annual discharge record. In both cases, discharge values for these rivers fell well within the regional discharge versus watershed area relationship (Figure S1), indicating that truncation of the data record did not have a major effect on annual discharge estimates. Watershed delineations were obtained directly from the Water Survey of Canada and used to calculate constituent yields as mass $\cdot$ m^{-2} $\cdot$ $year^{-1}$. Mean annual runoff was calculated in mm/year for each river using yearly discharge and the gross drainage areas described above.

3.3. Assessing Weathering Source Across Broad Geographic Regions

We assessed the weathering-derived source of alkalinity to each river using a modification of the inverse modeling approach of Gaillardet et al. (1999), which takes advantage of the fact that weathering of different rock types (e.g., carbonates versus silicates) results in the release of ions in characteristic ratios. The Gaillardet et al. (1999) mixing model takes the form (for X = Ca^{2+}, Mg^{2+}, and alkalinity):

$$\left(\frac{X}{Na}\right)_{river} = \sum_i \left(\frac{X}{Na}\right)_i \alpha_i(Na), \quad (2)$$

where *i* refers to the various end-member types and α_i are the mixing proportions of Na^+, which sum to 1. We used annual fluxes of Na^+, Ca^{2+}, Mg^{2+}, and alkalinity as model inputs and obtained end-members for carbonate, felsic silicate, and evaporite rocks from the literature (as outlined in Tank, Raymond, et al., 2012).

Models were run using an R version of the MixSIAR program (Stock & Semmens, 2016), which is a Bayesian mixing model that allows for the specification of end-member means and standard deviations, in addition to multiple mixture (here river water) data points, and iteratively generates a range of possible source contributions to the mixture (Moore & Semmens, 2008). We used the residual * process error structure and an uninformative prior and set the default number of iterations to *normal* unless the model did not converge, in which case iterations were increased. Model convergence was verified using the Gelman-Rubin diagnostic

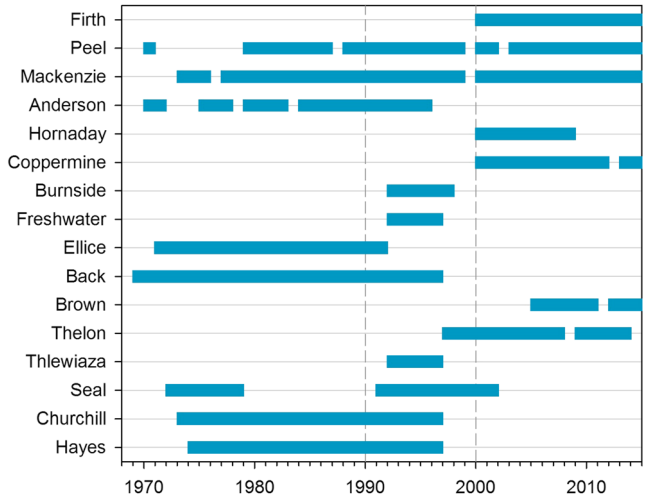

Figure 2. Length of record for each of the 16 study watersheds. The targeted "core period" is demarcated using dashed lines.

test. The model output was converted to source proportions of alkalinity using the various end-member alkalinity: Na^+ ratios. For each model output, the modeled Σ_i (alkalinity/Na^+)$_i$ was checked against the true, yearly alkalinity: Na^+ ratio.

3.4. Landscape Analyses and Extrapolation of DOC and Alkalinity Flux

We assessed landscape controls on DOC and alkalinity flux by examining the relationship between flow-weighted constituent concentrations and various landscape parameters. Watershed delineations, as described above, were used to calculate permafrost extent (Brown et al., 1998), soil organic carbon content to 1-m depth (Tarnocai et al., 2007), and catchment lithology (Jansen et al., 2010; Moosdorf et al., 2010) within each of the 16 study watersheds. Flow-weighted DOC and alkalinity were calculated as mean yearly constituent yield divided by mean yearly runoff. Relationships between landscape variables and flow-weighted concentrations were developed in the R statistical environment using the packages car and MASS (Fox & Weisberg, 2011; R Core Team, 2017; Venables & Ripley, 2002). Models were run iteratively using Akaike information criterion to select the best model fit. For the DOC model we considered mean annual runoff, soil organic carbon content, and various descriptors of permafrost extent (percent continuous, discontinuous, sporadic, and isolated, in addition to a combined metric of permafrost extent) as inputs to our model. For the alkalinity model we considered mean annual runoff, permafrost extent, and lithology (the SC, SS, SU, SM, and VB descriptors from Jansen et al. (2010) and Dürr et al. (2005)) as model inputs. Variance inflation factors were assessed for the models of best fit to ensure a lack of correlation between model coefficients.

Relationships between concentration and landscape parameters were further used to generate estimates of DOC and alkalinity export from the full Canadian Arctic drainage basin. To do this, we used the subset of sea basins outlined in Lammers et al. (2001) that are specific to the Canadian Arctic (Figure 1b). Sea basin delineations were obtained from the ArcticRIMS data portal (http://rims.unh.edu), and coverage of each of the above-described landscape characteristics was calculated for each sea basin. The relationships developed for estimating flow-weighted concentration from landscape characteristics were then applied to each of the sea basins, and sea basin-specific discharge values (Lammers et al., 2001) were used to estimate constituent flux.

4. Results and Discussion

4.1. Data Availability and Distribution

Although the 16 sites with paired streamflow and water chemistry data cover a broad swath of the western Arctic and sub-Arctic regions of Canada, they are biased toward locations in Yukon Territory and the mainland portions of the Northwest Territories and Nunavut (Figure 1). Some clear geographic gaps in stations that met our search criteria include the Nelson, which drains a large portion of land from the Rocky Mountains through the Canadian Prairie into Hudson Bay, and the presence of only two paired sites capturing flows from the Hudson Bay Lowland (Hayes and partially, the Churchill). Paired streamflow and chemistry data were not readily available for watersheds in Ontario or Quebec, which either do not have water quality data in the national network or have provincial monitoring efforts that focus on more southerly locations. Finally, there is only one station located within the Arctic Archipelago (Freshwater Creek), and it has a 5-year record of water chemistry. A number of gauging stations without coincident measures of water chemistry do exist (Table S1). These stations are predominately situated on the south and east shores of Hudson and James Bay, through Ungava Bay, and many are still active.

The period of record for the 16 sites begins as early as 1969 and extends to present day. However, not a single station provides an uninterrupted time series (Figure 2). Federal budget restraint measures in the mid-1990s resulted in the closure of several expensive water chemistry stations in Nunavut (e.g., Burnside), and leveraging of resources from Parks Canada which changed the geographic focus to sites within national parks

(e.g., Hornaday). The creation of the territory of Nunavut in 1992 was the justification for maintaining or beginning coordination of measurements on new territorial transboundary rivers such as the Coppermine and Thelon. Some stations are operated seasonally (e.g., Firth), with streamflow data only available from May to October each year. Because of the discontinuous nature of the overall record, we have centered our analyses on the years around 1990–1999, which is a core period for which most rivers have data, by using data from either directly within this time span, or the closest 5 years available. We use these core data for the bulk of our analyses (see the supporting information) to increase the robustness of comparisons among watersheds. Results from the full period of record and the exact date range of the core period for each river are presented in Table S2. An examination of constituent yields from the core period relative to the full period of record indicates that our approach provides a good estimate of mean annual exports and yields across these study systems (Figure S2). However, we do note that these rivers may be experiencing shifts in streamflow regimes (Déry et al., 2009; St. Jacques & Sauchyn, 2009) and biogeochemistry (Kicklighter et al., 2013; Tank et al., 2016) that we are unable to assess with currently available data and that the uncertainty of our estimates will be higher in rivers where the period of record is short.

4.2. Constituent Flux From Canadian Arctic Rivers Across Broad Geographic Scales

The watersheds with highest mean annual runoff were the Brown (361 mm) and Ellice (349 mm), followed by the Peel (301 mm; Table 1 and Figure 3). The former are relatively small watersheds in northeastern mainland Nunavut. The Peel is a mountainous watershed, which will enhance runoff over some of the more continental systems. The Back and Coppermine, for instance, have relatively lower runoff (146 and 179 mm, respectively) due to locations in central mainland Nunavut. One outlier is the Churchill, which is subject to significant diversions from its watershed to the Nelson to support hydropower generation in the latter. Of note is the Mackenzie, often the only completely Canadian watershed assessed in circumpolar studies (e.g., Holmes et al., 2012), which is among the rivers with the lowest average annual runoff (166 mm). Interannual variability in runoff was inversely related to the log of watershed size ($r^2 = 0.323$; $p = 0.027$ with the Churchill excluded; Figure S3), and as such, the series of smaller rivers in central Nunavut had higher year-to-year variability in runoff relative to other locations (Figure 3).

LOADEST models performed well for these rivers, with the r^2 of model outputs ranging from 78 to near 100%, and most models performing in the 90–100% range (Table S3). Mean annual yields of DOC ranged from lows of 26 mmol C $\cdot$ m^{-2} $\cdot$ year^{-1} on the Churchill to highs of 162 mmol C $\cdot$ m^{-2} $\cdot$ year^{-1} on the Peel (Figure 3). While there was a marginal tendency for mean annual inter-river DOC yields to increase with mean annual runoff (i.e., water yield: $r^2 = 0.21$, $p = 0.09$; see also Raymond et al., 2007; Figure 4), catchment characteristics such as soil organic carbon content and permafrost extent were also important drivers of between-catchment variation in DOC (see section 4.5). When plotted relative to runoff, DOC yields showed clear variation across the major physiographic regions in the study domain (Table 1 and Figures 1d and 4). Yields were lowest for rivers draining the central Canadian Shield (from the Coppermine in the west, to the Thlewiaza in the east; Table 1 and Figure 4) and highest for rivers draining the Cordillera, Interior Plains, and Hudson Bay Lowland (including the Seal, which drains organic rich terrain underlain by Canadian Shield). Rivers draining the central Canadian Shield also had markedly lower DOC yields when compared to large Arctic rivers from Alaska (the Yukon) and Siberia (the Ob' Yenisey, Lena, and Kolyma; Figure 4; Holmes et al., 2012), and—in general—smaller rivers draining the north Slope of Alaska (Figure 4; McClelland et al., 2014).

Mean annual yields for alkalinity also showed broad trends from west to east that tracked catchment physiography (Figure 3). Rivers draining the Cordillera and Interior Plains had relatively high alkalinity yields relative to runoff, while rivers draining the Canadian Shield had much lower area-normalized alkalinity exports (Figure 4). Alkalinity yields on Shield-draining systems were also low when compared to yields reported for the large Arctic rivers described above (Figure 4; Tank, Raymond, et al., 2012). Yields of Ca and Mg tracked alkalinity, reflecting differences in lithology across Shield, Plains, and Cordillera terrains (Figure 3). Sulfate yields were high (58–149 mmol $\cdot$ m^{-2} $\cdot$ year) in the Firth through Mackenzie basins but relatively low elsewhere (1–16 mmol $\cdot$ m^{-2} $\cdot$ year^{-1}; Figure 3). This geographic variation in SO_4 may reflect the distribution of sulfide minerals, which is proposed to shape the progression of weathering reactions in the Peel and Mackenzie catchments (Beaulieu et al., 2011; Calmels et al., 2007; Tank et al., 2016).

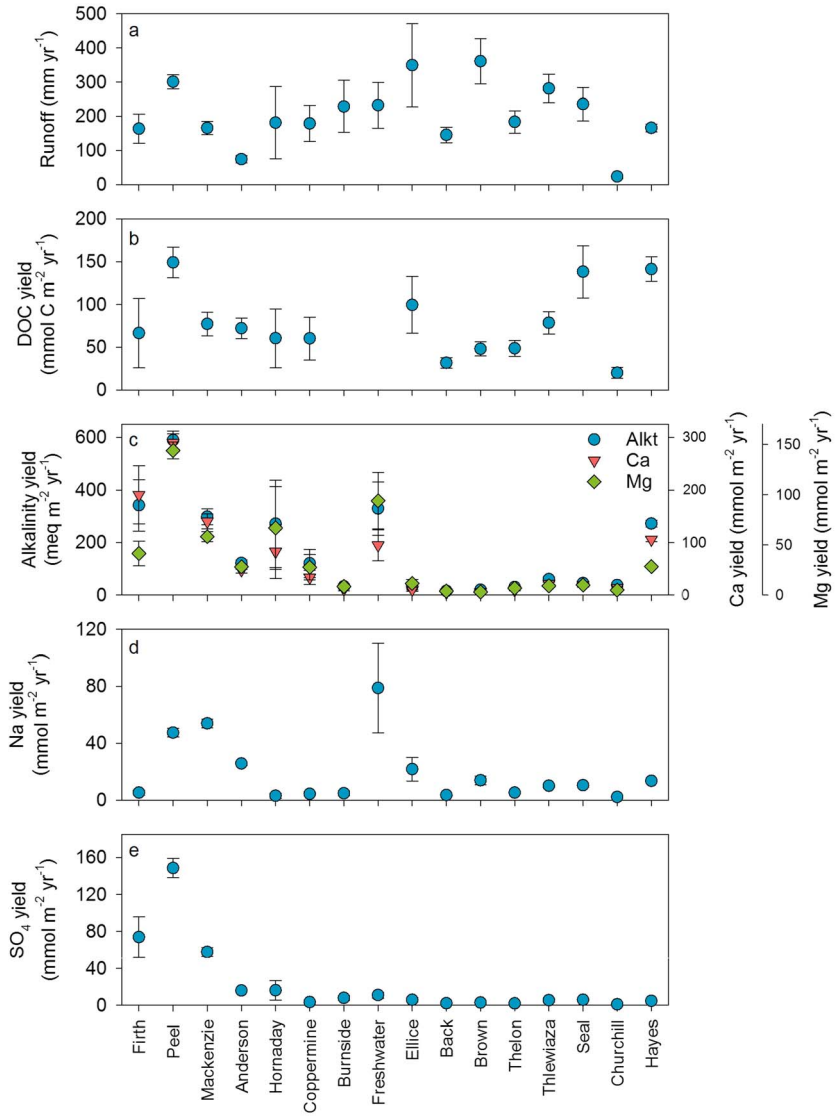

Figure 3. Water yield (runoff) and constituent yields for each of the study watersheds. The error bars show 95% confidence intervals around the mean.

This systematic variation in DOC and alkalinity yield across physiographic regions led to geographic variation in the relative contribution of organic versus inorganic species to total dissolved C export. Using alkalinity as a proxy for bicarbonate, we calculate that the non-CO_2 dissolved C flux (i.e., DOC plus non-CO_2 dissolved inorganic carbon) is dominated by inorganic species throughout the Firth to Coppermine Rivers in the west (Cordillera and Plains), and on the Churchill and Hayes Rivers in the east (Hudson Bay Lowland). In these systems, inorganic C accounts for 63–83% of dissolved C flux (Figures 3b and 3c). Conversely, in the central region of the Canadian Shield (Ellice to Seal Rivers) organic species dominate, comprising 56–78% of dissolved C flux. As described below, these differences can be expected to drive geographic variation in the effect of rivers on nearshore ecology and biogeochemistry across the Canadian Arctic.

4.3. Geographic Variation in the Seasonality of Constituent Flux and Concentration

The seasonality of DOC and alkalinity export varied markedly across the study catchments (Figure 5), in a manner that was consistent with the effects of latitude (temperature and permafrost extent) and variation in soils across physiographic region. Of the catchments for which we have full seasonal records (i.e., excluding the Firth and Hornaday), the Peel and Anderson through Brown Rivers are characterized by continuous

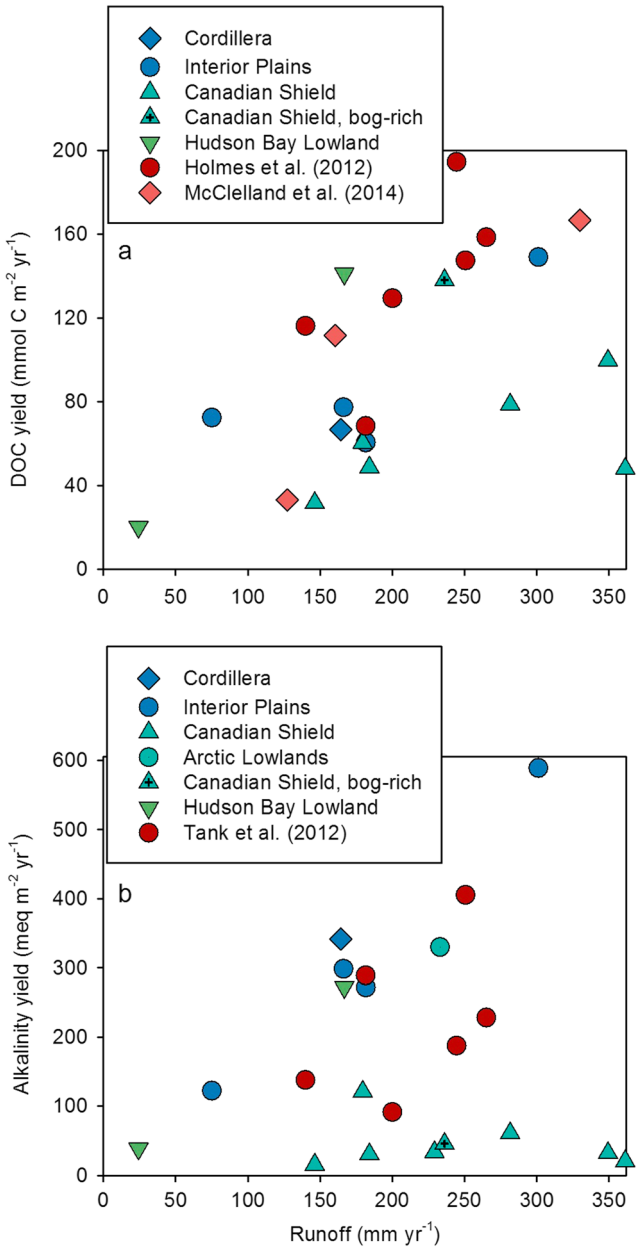

Figure 4. Comparison of dissolved organic carbon (DOC) and alkalinity yields relative to runoff, for results from this study and other major Arctic rivers. Plotted points from Holmes et al. (2012; DOC) and Tank, Raymond, et al., (2012; alkalinity) show yields for the Ob', Yenisey, Lena, Kolyma, Yukon, and Mackenzie Rivers. Plotted points from McClelland et al. (2014; DOC) show yields for the Sagavanirktok, Kuparuk, and Colville Rivers. Yields from this study are demarcated by major physiographic region.

permafrost coverage at, or near 100% (Figure 1 and Table 1). These systems display clear nival hydrologic regimes, with discharge, and thus constituent export returning to near-zero during the winter months. As a result, these enorthernmost systems are characterized by a constituent export regime that is dominated by a short summer season, with a two calendar month period (May–June or June–July) providing between 42% (for DOC on the Peel) and 79% (for alkalinity on the Ellice) of total annual exports from these systems. In contrast, rivers draining more southerly watersheds exhibit constituent export that is much more evenly distributed across seasons, with export continuing throughout winter months, and modest summertime peaks (Figure 5).

In addition, seasonal variation in DOC export relative to alkalinity export varied according to physiographic region. For example, rivers draining the Interior Plains (Peel through Anderson) had proportionately greater DOC export during the high flow summer months but greater relative alkalinity export during the receding limb of the hydrograph through autumn (Figure 5). This pattern likely reflects changing flow paths with season, with water tending to be routed over surficial, organic-rich soils during the high flow spring-summer months (Townsend-Small et al., 2011), but increasingly accessing the deeper mineral soils of this region as the thaw season progresses (e.g., Quinton & Pomeroy, 2006). Elsewhere, seasonal patterns in relative DOC and alkalinity export are near identical, reflecting the shallow, poorly developed soils of the Canadian Shield (Ellice through Thlewiaza) and the deep, organic-rich soils of the Hudson Bay Lowland (Hugelius et al., 2014).

These patterns in export seasonality (Figure 5) also track geographic variation in the seasonality of DOC and alkalinity concentration (Figure 6). On the Interior Plains, for example, alkalinity shows a clear dilution during the high flows of spring, while DOC concentrations are higher during spring freshet relative to other times of year (Figures 6a and 6b). In contrast, DOC and alkalinity concentrations are relatively consistent through the year on the Canadian Shield and Hudson Bay Lowland. Regional differences in overall concentration also occur. Alkalinity is relatively high on the Interior Plains and Hudson Bay Lowland, but low on the Canadian Shield (Figure 6). For DOC, concentrations also tend to be relatively low on the Canadian Shield but are higher on the Interior Plains, and in particular on the Hudson Bay Lowland. In general, these patterns track physiographic differences in lithology and soil organic matter across the study domain.

4.4. Provenance of Weathering Ions Across the Canadian Arctic Domain

Plots of ion ratios indicate geographic shifts in the dominant source of weathering ions, as expected given the lithologic variation throughout the Canadian Arctic drainage basin. Weathering ions appear to be largely carbonate rock derived in the west (Cordillera and Interior Plains) and eastern-most (Hudson Bay Lowland) regions of the study domain, and largely silicate derived over central (Shield) terrains (Figures 7a and 7b). In particular, the Firth, Peel, Hornaday, Coppermine, Churchill, and Hayes Rivers exhibit ion ratios indicative of weathering inputs dominated by carbonate rocks (Figures 7a and 7b), while the Burnside through Seal Rivers exhibit ratios more indicative of silicate lithologies. Even within Shield regions, however, small contributions from carbonates can cause carbonate rock to become a near-dominant provider of overall alkalinity to these systems (Figure 7c).

In addition to understanding ionic provenance, Na-specific ratios can be used to estimate CO_2 consumption by weathering over broad spatial scales (e.g., following Gaillardet et al., 1999). We assume that—over

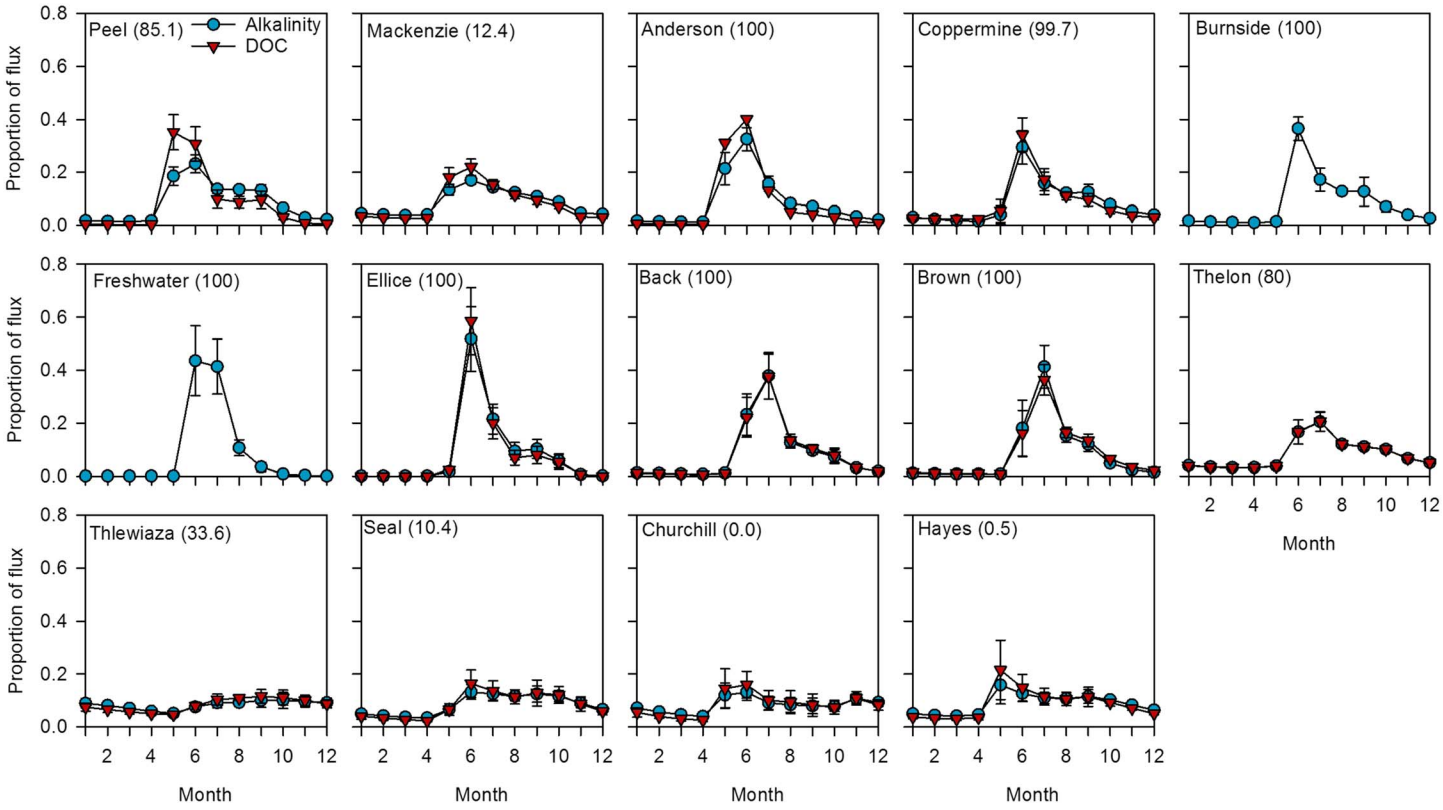

Figure 5. Monthly climatologies of dissolved organic carbon (DOC) and alkalinity flux, showing the proportion of flux occurring within each of 12 monthly bins. The percentage of each catchment underlain by continuous permafrost is shown in brackets. Climatologies were calculated using each year within the core data period, as the proportion of yearly flux occurring in any given month. The error bars indicate the standard error of the mean.

contemporary time scales—silicate rock weathering by carbonic acid consumes one mole of CO_2 for each mole of bicarbonate produced, while carbonate rock weathering by carbonic acid consumes one mole of CO_2 for every two moles of bicarbonate produced. Equations (3) and (4) show this stoichiometry for generalized silicate (wollastonite) and dolomite, respectively:

$$CaSiO_3 + 2CO_2 + H_2O \rightarrow Ca^{2+} + 2HCO_3^- + SiO_2 \quad (3)$$

$$CaMg(CO_3)_2 + 2CO_2 + 2H_2O \rightarrow Ca^{2+} + Mg^{2+} + 4HCO_3^- \quad (4)$$

We also assume that sulfate in this region may be derived from the oxidation of sulfide minerals, following the broad distribution of sulfides throughout the western Canadian Arctic (Beaulieu et al., 2011; Calmels et al., 2007; Tank et al., 2016), and therefore calculate a range of values with, and without, consideration of sulfide oxidation. The sulfuric acid that results from this oxidation reaction (e.g., equation (5)) enables the production of bicarbonate in the absence of CO_2 fixation (equation (6)), and—over millennial time scales—acts as a positive feedback to climate change (Berner & Berner, 2012).

$$FeS_2 + \frac{15}{4}O_2 + \frac{7}{2}H_2O \rightarrow Fe(OH)_3 + 2H_2SO_4 \quad (5)$$

$$CaMg(CO_3)_2 + H_2SO_4 \rightarrow Ca^{2+} + Mg^{2+} + 2HCO_3^- + SO_4^{2-} \quad (6)$$

Our mixing model estimates (Figure 7c) indicate that the approximate 2.3×10^2 meq $\cdot$ m^{-2} $\cdot$ year^{-1} of alkalinity export from our study watersheds (calculated as a per-area yield, with total alkalinity export normalized to total watershed area) is derived from $0.8 - 1.2 \times 10^2$ mmol $\cdot$ m^{-2} $\cdot$ year^{-1} of CO_2 fixation and $1.1 - 1.5 \times 10^2$ mmol $\cdot$ m^{-2} $\cdot$ year^{-1} of rock dissolution. Silicate weathering accounts for less than 30% of the total CO_2 consumption, while sulfide oxidation — with 98% of SO_4 originating in the Firth through

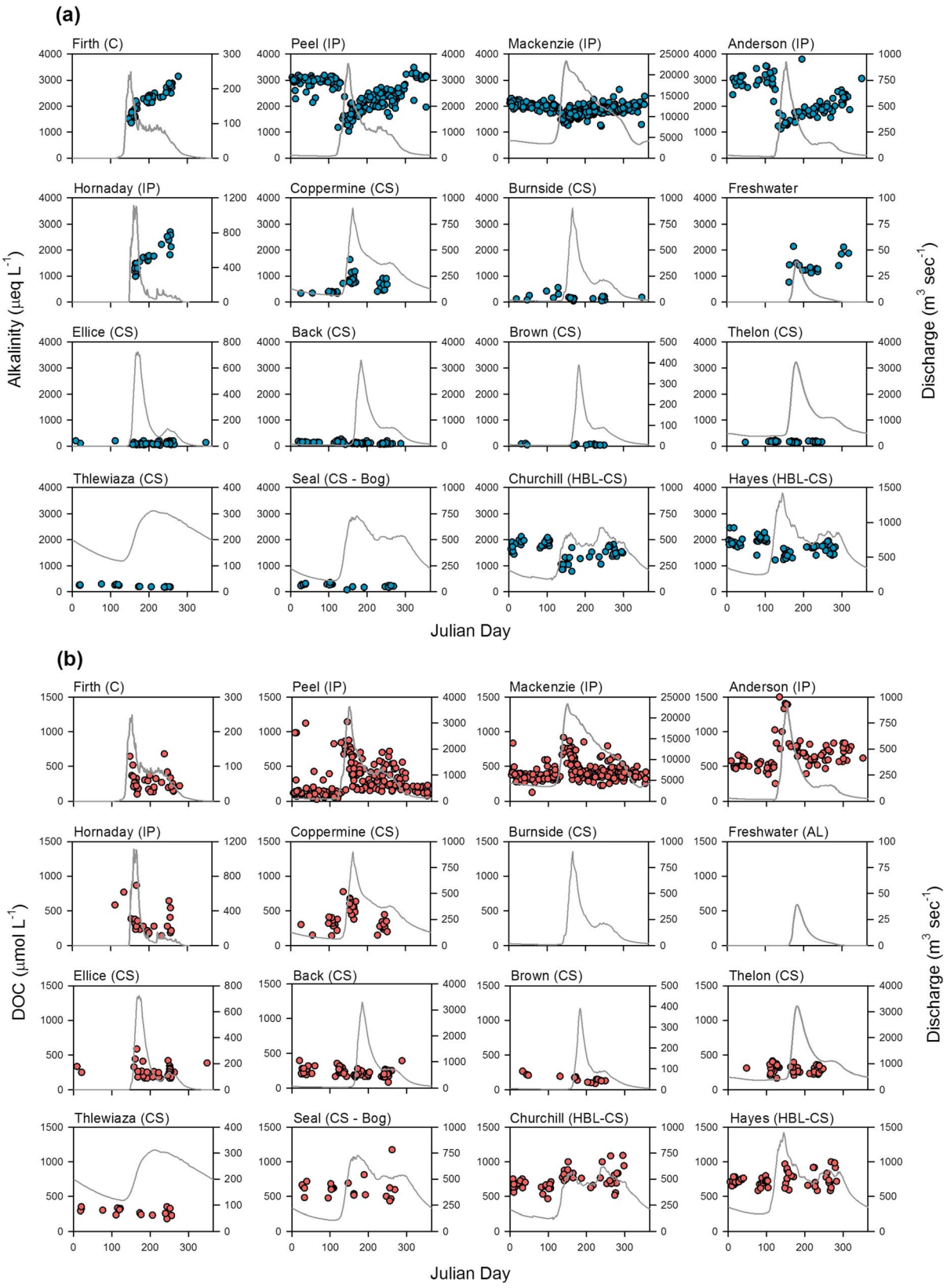

Figure 6. Plots of (a) alkalinity and (b) dissolved organic carbon (DOC) concentration relative to mean daily discharge over the full period of record. All available concentrations are plotted by Julian day. No DOC data are available for the Burnside River and Freshwater Creek. Physiographic region is indicated following the legend in Figure 1.

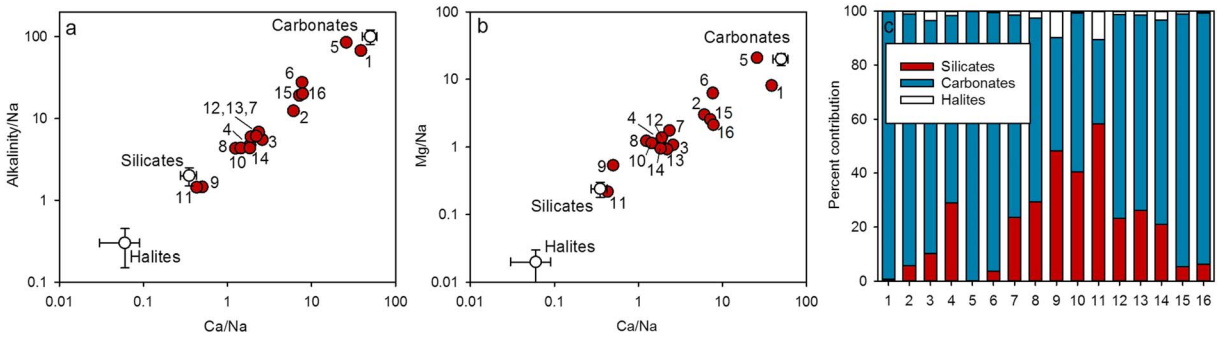

Figure 7. Mixing model to indicate weathering sources of alkalinity. Across all panels, rivers are indicated as follows: 1: Firth, 2: Peel, 3: Mackenzie, 4: Anderson, 5: Hornaday, 6: Coppermine, 7: Burnside, 8: Freshwater, 9: Ellice, 10: Back, 11: Brown, 12: Thelon, 13: Thlewiaza, 14: Seal, 15: Churchill, 16: Hayes.

Anderson watersheds—accounts for as much as half of the rock-derived bicarbonate. This compares to an area-weighted DOC export of 0.7×10^2 mmol · m^{-2} · $year^{-1}$. Thus, the bulk dissolved carbon export from these river systems appears to represent a net transfer of carbon from terrestrial reservoirs to the atmosphere, following the apparent mineralization of the majority of river-mouth DOC in the Arctic Ocean (Alling et al., 2010; Mann et al., 2016), and—over millennial time scales—the eventual oceanic precipitation of rock-derived bicarbonate (Berner & Berner, 2012). Given that both DOC mobilization and sulfide oxidation may be increasing in Canada's north (e.g., Tank et al., 2016), the rate at which this transfer is occurring may not be static.

4.5. Extrapolating Constituent Flux to the Greater Canadian Arctic Domain

In the absence of coupled water chemistry and discharge measures for broad expanses of the Canadian Arctic, quantifying constituent export requires some degree of extrapolation (e.g., Holmes et al., 2012). Using flow-weighted concentrations for our extrapolation efforts, we found that both DOC and alkalinity could be predicted relatively well from landscape variables, with models of best fit explaining 72% of between-catchment variation in flow-weighted DOC ($r^2 = 0.724$, $p = 0.004$), and 96% of variation in flow-weighted alkalinity ($r^2 = 0.960$, $p < 0.001$; Table 2). These general models (Table 2) show alkalinity to increase significantly with increasing coverage of sedimentary rocks (Moosdorf et al., 2011; Tank, Raymond, et al.,

Table 2
Outputs From the Landscape Analysis

	Alkalinity (ueq · L^{-1})				DOC (uM)		
	Estimate	*t*	*p*		Estimate	*t*	*p*
Intercept	−99.71	−0.95	0.369	Intercept	536.25	3.44	0.006
SC	16.85	7.88	<0.001	Runoff	−0.75	−1.49	0.167
SM	12.07	3.53	0.006	SOC	11.67	2.91	0.015
SS	16.38	4.81	0.001	Continuous	−2.50	−2.43	0.036
SU	95.84	3.86	0.004				
VB	62.79	1.74	0.115				
Sporadic	16.80	4.76	0.001				

	Alkalinity (Geq · $year^{-1}$)	DOC (Gmol · $year^{-1}$)
Beaufort Sea	735 (43)	257 (26)
Arctic Archipelago	153 (15)	82 (10)
Hudson Bay	794 (98)	379 (39)
Hudson Strait	152 (27)	68 (37)
Total	1834	785

Note. The top panel shows the results of the regression analysis; the bottom panel shows extrapolation to sea basins, with the standard error of individual estimates shown in brackets. Model statistics are as follows: alkalinity $r^2 = 0.960$, $p < 0.001$; DOC $r^2 = 0.724$, $p = 0.004$. SC, SM, SS, SU, and VB indicate percent carbonate sedimentary rocks, mixed sedimentary rocks, siliciclastic sedimentary rocks, unconsolidated sediments, and basic volcanic rocks, respectively (Dürr et al., 2005; Jansen et al., 2010); sporadic and continuous refer to permafrost extent (Brown et al., 1998), SOCC indicates mean soil organic carbon content in kg m^{-2} in the top 1 m of soil (Tarnocai et al., 2007).

2012) and more marginally with basalts (Dessert et al., 2003), consistent with the increased weatherability of both rock types and high carbonate content of sedimentary lithologies. Flow weighted DOC increased with increasing soil organic carbon content (Tank, Frey, et al., 2012), and showed a nonsignificant, but negative, relationship with runoff, likely as a result of the relatively high runoff over much of the low-DOC Canadian Shield (Figure 3). Both alkalinity and DOC increased with decreasing permafrost extent, expressed as a negative relationship between DOC and continuous permafrost coverage, and a positive relationship between alkalinity and sporadic (i.e., near absent) permafrost. For alkalinity, this relationship is consistent with deepening flow paths increasing contact between water and mineral soils and the effect of temperature on processes associated with weathering (Beaulieu et al., 2012; Tank, Frey, et al., 2012), in addition to the large proportion of Shield catchments underlain by near-100% permafrost (the Burnside, Ellice, Back, and Brown). For DOC, this relationship may be more reflective of the higher fraction of peatlands in catchments with lower permafrost coverage (the Seal, Hayes, and Churchill), and poor soil development in Shield catchments where continuous permafrost is near 100%.

These broad relationships allow us to extrapolate DOC and alkalinity export across the major sea basins that constitute the Canadian Arctic drainage basin (Figure 1b). In total, we estimate exports of 1,800 Geq/year for alkalinity and 800 Gmol/year for DOC (Table 2). When considered in bulk, these estimates compare well to past estimates for alkalinity, including those of Tank, Raymond, et al., (2012; 1,820 Geq/year for all DIC species) and Alkire et al. (2017; 640–680 Geq/year for just the Beaufort and Arctic Archipelago sea basins). For DOC, our estimates were somewhat higher than previous estimates, including those of McGuire et al. (2010; 670 Gmol/year) and Kicklighter et al. (2013; 550 Gmol/year), who used the Terrestrial Ecosystem Model to simulate DOC loading throughout the Arctic basin, and Manizza et al. (2009; 750 Gmol/year), who performed a discharge-based extrapolation from large river estimates of flux. These new estimates of carbon flux for vast ungauged areas of the Canadian Arctic provide a valuable tool for extrapolation to other ungauged areas and appear to be particularly robust for alkalinity. However, they may also be sensitive to the large gaps in data coverage through the Arctic Archipelago and east shores of Hudson Bay. Future targeted sampling efforts in regions with poor data coverage will help to further refine, and increase our confidence in estimates of the oceanward flux of biogeochemical constituents throughout the Canadian Arctic.

5. Study Implications and General Conclusions

More than three-quarters of the Canadian landmass drains north to enter the Arctic Ocean and Hudson Bay. The water transported by these drainages can, in turn, fundamentally shape the ecology and biogeochemistry of the nearshore Arctic Ocean. For example, riverine organic carbon provides a subsidy to bolster nearshore microbial metabolism (Ortega-Retuerta et al., 2012), while the concentration of, and balance between, organic and inorganic species plays a key role in determining the buffering capacity of nearshore waters (Chierici & Fransson, 2009; Mathis et al., 2011). From available data, we document that this balance shows fundamental, but predictable, geographic, and seasonal shifts throughout the Canadian Arctic domain, with Cordillera and Plains rivers that are well buffered relative to seawater during the summer, fall and winter, but more dilute during the spring freshet, and Shield rivers that show almost no alkalinity-based buffering capacity, but contain notable amounts of DOC that may be rapidly mineralized to cause further declines in alkalinity across estuarine gradients (Semiletov et al., 2016).

Superimposed on this geographic and seasonal variation are the long-term trends in organic and inorganic processes that have been documented in some Canadian Arctic locations (e.g., Spence et al., 2015; Tank et al., 2016; Wauthy et al., 2018). Such increases in DOC mobilization and processes such as pyrite-induced bicarbonate mobilization have the potential to substantially alter the chemical composition of water flowing from land to ocean in Canada's north, and fundamentally affect the aquatic carbon cycle across land-ocean gradients. Despite this, we document that the collection of river water chemistry measurements is patchy throughout much of the Canadian Arctic domain, with records from only two watersheds (the Mackenzie and the Peel) that range over long enough time scales to evaluate long-term change (see also Kokelj et al., 2013; Tank et al., 2016). As a result, Canada is unable to assess the current state of freshwater fluxes throughout much of the Canadian Arctic and Hudson Bay drainage basins or determine whether these fluxes are changing. This need is particularly pronounced for the Arctic Archipelago, which is unique in its physiography

compared to the more southerly regions that dominate this assessment, and the east shores of Hudson Bay, where runoff (Statistics Canada, 2017) and soil organic carbon stocks (Hugelius et al., 2014) are greater than in more westerly regions of the Canadian Shield. Throughout the Arctic Ocean drainage, the collection of coupled measures of discharge and water chemistry, across a distributed array of watersheds, remains a clear priority for understanding northern change.

Acknowledgments
Funding for this work was provided by Environment and Climate Change Canada and the Campus Alberta Innovates Program. We would like to thank the many individuals from the Water Survey of Canada and Environment and Climate Change Canada whose data collection efforts made this work possible. Minzhen Su and Jasmine Waltho assisted with data access. Chemistry data used in our analyses are provided in the supporting information. Discharge data are publicly available online from the Water Survey of Canada (https://wateroffice.ec.gc.ca/).

References

Alkire, M. B., Jacobson, A. D., Lehn, G. O., Macdonald, R. W., & Rossi, M. W. (2017). On the geochemical heterogeneity of rivers draining into the straits and channels of the Canadian Arctic Archipelago. *Journal of Geophysical Research: Biogeosciences*, *122*, 2527–2547. https://doi.org/10.1002/2016JG003723

Alling, V., Sanchez-Garcia, L., Porcelli, D., Pugach, S., Vonk, J. E., van Dongen, B., et al. (2010). Nonconservative behavior of dissolved organic carbon across the Laptev and East Siberian seas. *Global Biogeochemical Cycles*, *24*, GB4033. https://doi.org/10.1029/2010GB003834

Beaulieu, E., Godderis, Y., Donnadieu, Y., Labat, D., & Roelandt, C. (2012). High sensitivity of the continental-weathering carbon dioxide sink to future climate change. *Nature Climate Change*, *2*(5), 346–349. https://doi.org/10.1038/nclimate1419

Beaulieu, E., Godderis, Y., Labat, D., Roelandt, C., Calmels, D., & Gaillardet, J. (2011). Modeling of water-rock interaction in the Mackenzie basin: Competition between sulfuric and carbonic acids. *Chemical Geology*, *289*(1–2), 114–123. https://doi.org/10.1016/j.chemgeo.2011.07.020

Berner, E. K., & Berner, R. A. (2012). *Global environment: Water, air, and geochemical cycles* (2nd ed.). Princeton, NJ: Princeton University Press.

Booth, G., Raymond, P. A., & Oh, N.-H. (2007). *LoadRunner, software and website*. New Haven, CT: Yale University.

Brown, J., Ferrians, O. J. Jr., Heginbottom, J. A., & Melnikov, E. S. (1998). *Circum-arctic map of permafrost and ground ice conditions*. Boulder, CO: National Snow and Ice Data Center/World Data Center for Glaciology.

Burnham, K. P., & Anderson, D. R. (2002). *Model selection and multi-model inference: A practical information-theoretic approach*. New York, NY: Springer.

Calmels, D., Gaillardet, J., Brenot, A., & France-Lanord, C. (2007). Sustained sulfide oxidation by physical erosion processes in the Mackenzie River basin: Climatic perspectives. *Geology*, *35*(11), 1003–1006. https://doi.org/10.1130/g24132a.1

Chierici, M., & Fransson, A. (2009). Calcium carbonate saturation in the surface water of the Arctic Ocean: Undersaturation in freshwater influenced shelves. *Biogeosciences*, *6*(11), 2421–2431. https://doi.org/10.5194/bg-6-2421-2009

Clayton, J. S., Ehrlich, W. A., Cann, D. B., Day, J. H., & Marshall, I. B. (1977). *Soils of Canada*. Ottawa, ON: Agriculture Canada, Research Branch.

Connolly, C. T., Khosh, M. S., Burkart, G. A., Douglas, T. A., Holmes, R. M., Jacobson, A. D., et al. (2018). Watershed slope as a predictor of fluvial dissolved organic matter and nitrate concentrations across geographical space and catchment size in the Arctic. *Environmental Research Letters*, *13*(10), 104015. https://doi.org/10.1088/1748-9326/aae35d

Crawford, J. (2015). Appendix 4.3 B: An assessment of the hydraulic impacts of the Churchill River diversion on the upper and lower Churchill Rivers in *Regional Cumulative Effects Assessments for Hydroelectric Developments on the Churchill, Brentwood, and Nelson River Systems: Phase II Report*. Manitoba Hydro.

Déry, S. J., Hernandez-Henriquez, M. A., Burford, J. E., & Wood, E. F. (2009). Observational evidence of an intensifying hydrological cycle in northern Canada. *Geophysical Research Letters*, *36*, L13402. https://doi.org/10.1029/2009GL038852

Dessert, C., Dupre, B., Gaillardet, J., Francois, L. M., & Allegre, C. J. (2003). Basalt weathering laws and the impact of basalt weathering on the global carbon cycle. *Chemical Geology*, *202*(3–4), 257–273. https://doi.org/10.1016/j.chemgeo.2002.10.001

Drake, T. W., Raymond, P. A., & Spencer, R. G. M. (2017). Terrestrial carbon inputs to inland waters: A current synthesis of estimates and uncertainty. *Limnology and Oceanography Letters*, *3*(3), 132–142. https://doi.org/10.1002/lol2.10055

Dürr, H. H., Meybeck, M., & Dürr, S. H. (2005). Lithologic composition of the Earth's continental surfaces derived from a new digital map emphasizing riverine material transfer. *Global Biogeochemical Cycles*, *19*, GB4S10. https://doi.org/10.1029/2005GB002515

Fenton, M. M., Schreiner, B. T., Nielsen, E., & Pawlowicz, J. G. (1994). Quaternary geology of the Western Plains. In G. D. Mossop & I. Shetsen (Eds.), *Geological Atlas of the Western Canada Sedimentary Basin* (pp. 413–420). Canada: Canadian Society of Petroleum Geologists and Alberta Research Council.

Fox, J., & Weisberg, S. (2011). *An R companion to applied regression* (2nd ed.). Thousand Oaks, CA: Sage.

Gaillardet, J., Dupre, B., Louvat, P., & Allegre, C. J. (1999). Global silicate weathering and CO_2 consumption rates deduced from the chemistry of large rivers. *Chemical Geology*, *159*(1–4), 3–30. https://doi.org/10.1016/S0009-2541(99)00031-5

Godin, P., Macdonald, R. W., Kuzyk, Z. Z. A., Goñi, M. A., & Stern, G. A. (2017). Organic matter compositions of rivers draining into Hudson Bay: Present-day trends and potential as recorders of future climate change. *Journal of Geophysical Resesarch: Biogeosciences*, *122*, 1848–1869. https://doi.org/10.1002/2016JG003569

Harms, T. K., Edmonds, J. W., Genet, H., Creed, I. F., Aldred, D., Balser, A., & Jones, J. B. (2016). Catchment influence on nitrate and dissolved organic matter in Alaskan streams across a latitudinal gradient. *Journal of Geophysical Research: Biogeosciences*, *121*, 350–369. https://doi.org/10.1002/2015JG003201

Holmes, R. M., Coe, M. T., Fiske, G. J., Gurtovaya, T., McClelland, J. W., Shiklomanov, A. I., et al. (2013). Climate change impacts on the hydrology and biogeochemistry of Arctic Rivers. In C. R. Goldman, M. Kumagi, & R. D. Robarts (Eds.), *Climatic change and global warming of inland waters: Impacts and mitigation for ecosystems and societies* (pp. 3–26). Oxford, UK: Wiley-Blackwell.

Holmes, R. M., McClelland, J. W., Peterson, B. J., Tank, S. E., Bulygina, E., Eglinton, T. I., et al. (2012). Seasonal and annual fluxes of nutrients and organic matter from large rivers to the Arctic Ocean and surrounding seas. *Estuaries and Coasts*, *35*(2), 369–382. https://doi.org/10.1007/s12237-011-9386-6

Hugelius, G., Strauss, J., Zubrzycki, S., Harden, J. W., Schuur, E. A. G., Ping, C. L., et al. (2014). Estimated stocks of circumpolar permafrost carbon with quantified uncertainty ranges and identified data gaps. *Biogeosciences*, *11*(23), 6573–6593. https://doi.org/10.5194/bg-11-6573-2014

Jansen, N., Hartmann, J., Lauerwald, R., Dürr, H. H., Kempe, S., Loos, S., & Middelkoop, H. (2010). Dissolved silica mobilization in the conterminous USA. *Chemical Geology*, *270*(1-4), 90–109. https://doi.org/10.1016/j.chemgeo.2009.11.008

Johnston, S. E., Shorina, N., Bulygina, E., Vorobjeva, T., Chupakova, A., Klimov, S. I., et al. (2018). Flux and seasonality of dissolved organic matter from the Northern Dvina (Severnaya Dvina) River, Russia. *Journal of Geophysical Research: Biogeosciences*, *123*, 1041–1056. https://doi.org/10.1002/2017JG004337

Kicklighter, D. W., Hayes, D. J., McClelland, J. W., Peterson, B. J., McGuire, A. D., & Melillo, J. M. (2013). Insights and issues with simulating terrestrial DOC loading of Arctic river networks. *Ecological Applications*, *23*(8), 1817–1836. https://doi.org/10.1890/11-1050.1

Kokelj, S. V., Lacelle, D., Lantz, T. C., Tunnicliffe, J., Malone, L., Clark, I. D., & Chin, K. S. (2013). Thawing of massive ground ice in mega slumps drives increases in stream sediment and solute flux across a range of watershed scales. *Journal of Geophysical Research: Earth Surface*, *118*, 681–692. https://doi.org/10.1002/jgrf.20063

Lammers, R. B., Shiklomanov, A. I., Vorosmarty, C. J., Fekete, B. M., & Peterson, B. J. (2001). Assessment of contemporary Arctic river runoff based on observational discharge records. *Journal of Geophysical Research*, *106*(D4), 3321–3334. https://doi.org/10.1029/2000JD900444

Manizza, M., Follows, M. J., Dutkiewicz, S., McClelland, J. W., Menemenlis, D., Hill, C. N., et al. (2009). Modeling transport and fate of riverine dissolved organic carbon in the Arctic Ocean. *Global Biogeochemical Cycles*, *23*, GB4006. https://doi.org/10.1029/2008GB003396

Mann, P. J., Spencer, R. G. M., Hernes, P. J., Six, J., Aiken, G. R., Tank, S. E., et al. (2016). Pan-arctic trends in terrestrial dissolved organic matter from optical measurements. *Frontiers in Earth Science*, *4*, 25. https://doi.org/10.3389/feart.2016.00025

Martini, I. P. (1989). The Hudson Bay Lowland: Major geologic features and assets. In W. J. M. van der Linden, et al. (Eds.), *Coastal Lowlands* (pp. 25–34). Dordrecht: Springer.

Mathis, J. T., Cross, J. N., & Bates, N. R. (2011). Coupling primary production and terrestrial runoff to ocean acidification and carbonate mineral suppression in the eastern Bering Sea. *Journal of Geophysical Research*, *116*, C02030. https://doi.org/10.1029/2010JC006453

McClelland, J. W., Holmes, R. M., Dunton, K. H., & Macdonald, R. W. (2012). The Arctic Ocean estuary. *Estuaries and Coasts*, *35*(2), 353–368. https://doi.org/10.1007/s12237-010-9357-3

McClelland, J. W., Tank, S. E., Spencer, R. G. M., & Shiklomanov, A. I. (2015). Coordination and sustainability of river observing activities in the Arctic. *Arctic*, *68*(5), 59–68. https://doi.org/10.14430/arctic4448

McClelland, J. W., Townsend-Small, A., Holmes, R. M., Pan, F., Stieglitz, M., Khosh, M., & Peterson, B. J. (2014). River export of nutrients and organic matter from the North Slope of Alaska to the Beaufort Sea. *Water Resources Research*, *50*, 1823–1839. https://doi.org/10.1002/2013WR014722

McGuire, A. D., Hayes, D. J., Kicklighter, D. W., Manizza, M., Zhuang, Q., Chen, M., et al. (2010). An analysis of the carbon balance of the Arctic Basin from 1997 to 2006. *Tellus B*, *62*(5), 455–474. https://doi.org/10.1111/j.1600-0889.2010.00497.x

Moore, J. W., & Semmens, B. X. (2008). Incorporating uncertainty and prior information into stable isotope mixing models. *Ecology Letters*, *11*(5), 470–480. https://doi.org/10.1111/j.1461-0248.2008.01163.x

Moosdorf, N., Hartmann, J., & Dürr, H. H. (2010). Lithological composition of the North American continent and implications of lithological map resolution for dissolved silica flux modeling. *Geochemistry, Geophysics, Geosystems*, *11*, Q11003. https://doi.org/10.1029/2010GC003259

Moosdorf, N., Hartmann, J., Lauerwald, R., Hagedorn, B., & Kempe, S. (2011). Atmospheric CO_2 consumption by chemical weathering in North America. *Geochimica et Cosmochimica Acta*, *75*(24), 7829–7854. https://doi.org/10.1016/j.gca.2011.10.007

Ortega-Retuerta, E., Jeffrey, W. H., Babin, M., Bélanger, S., Benner, R., Marie, D., et al. (2012). Carbon fluxes in the Canadian Arctic: Patterns and drivers of bacterial abundance, production and respiration on the Beaufort Sea margin. *Biogeosciences*, *9*(9), 3679–3692. https://doi.org/10.5194/bg-9-3679-2012

Quinton, W. L., Hayashi, M., & Pietroniro, A. (2003). Connectivity and storage functions of channel fens and flat bogs in northern basins. *Hydrological Processes*, *17*(18), 3665–3684. https://doi.org/10.1002/hyp.1369

Quinton, W. L., & Pomeroy, J. W. (2006). Transformations of runoff chemistry in the Arctic tundra, Northwest Territories, Canada. *Hydrological Processes*, *20*(14), 2901–2919. https://doi.org/10.1002/hyp.6083

R Core Team (2017). *R: A language and environment for statistical computing*. Vienna, Austria: R Foundation for Statistical Computing.

Raymond, P. A., McClelland, J. W., Holmes, R. M., Zhulidov, A. V., Mull, K., Peterson, B. J., et al. (2007). Flux and age of dissolved organic carbon exported to the Arctic Ocean: A carbon isotopic study of the five largest arctic rivers. *Global Biogeochemical Cycles*, *21*, GB4011. https://doi.org/10.1029/2007GB002934

Runkel, R. L., Crawford, C. G., & Cohn, T. A. (2004). *Load Estimator (LOADEST): A FORTRAN program for estimating constituent loads in streams and rivers*. Reston, VA: U.S. Geological Survey Techniques and Methods Book 4, Chapter A5.

Semiletov, I., Pipko, I., Gustafsson, Ö., Anderson, L. G., Sergienko, V., Pugach, S., et al. (2016). Acidification of East Siberian Arctic Shelf waters through addition of freshwater and terrestrial carbon. *Nature Geoscience*, *9*(5), 361–365. https://doi.org/10.1038/ngeo2695

Soil Landscapes of Canada Working Group (2010). Soil landscapes of Canada version 3.2, digital map and database at 1:1 million scale, Agriculture and Agri-Food Canada.

Spence, C., & Burke, A. (2008). Estimates of Canadian Arctic Archipelago runoff from observed hydrometric data. *Journal of Hydrology*, *362*(3-4), 247–259. https://doi.org/10.1016/j.jhydrol.2008.08.019

Spence, C., Kokelj, S. V., Kokelj, S. A., McCluskie, M., & Hedstrom, N. (2015). Evidence of a change in water chemistry in Canada's subarctic associated with enhanced winter streamflow. *Journal of Geophysical Research: Biogeosciences*, *120*, 113–127. https://doi.org/10.1002/2014JG002809

St. Jacques, J. M., & Sauchyn, D. J. (2009). Increasing winter baseflow and mean annual streamflow from possible permafrost thawing in the Northwest Territories, Canada. *Geophysical Research Letters*, *36*, L01401. https://doi.org/10.1029/2008GL035822

Statistics Canada (2017). Human Activity and the Environment: Freshwater in Canada. Minister of Industry. Retrieved from https://www150.statcan.gc.ca/n1/pub/16-201-x/16-201-x2017000-eng.htm on August 21, 2018.

Stock, B. C., & Semmens, B. X. (2016). Unifying error structures in commonly used biotracer mixing models. *Ecology*, *97*(10), 2562–2569. https://doi.org/10.1002/ecy.1517

Tank, S. E., Fellman, J. B., Hood, E., & Kritzberg, E. S. (2018). Beyond respiration: Controls on lateral carbon fluxes across the terrestrial-aquatic interface. *Limnology and Oceanography Letters*, *3*(3), 76–88. https://doi.org/10.1002/lol2.10065

Tank, S. E., Frey, K. E., Striegl, R. G., Raymond, P. A., Holmes, R. M., McClelland, J. W., & Peterson, B. J. (2012). Landscape-level controls on dissolved carbon flux from diverse catchments of the circumboreal. *Global Biogeochemical Cycles*, *26*, GB0E02. https://doi.org/10.1029/2012GB004299

Tank, S. E., Raymond, P. A., Striegl, R. G., McClelland, J. W., Holmes, R. M., Fiske, G. J., & Peterson, B. J. (2012). A land-to-ocean perspective on the magnitude, source and implication of DIC flux from major Arctic rivers to the Arctic Ocean. *Global Biogeochemical Cycles*, *26*, GB4018. https://doi.org/10.1029/2011GB004192

Tank, S. E., Striegl, R. G., McClelland, J. W., & Kokelj, S. V. (2016). Multi-decadal increases in dissolved organic carbon and alkalinity flux from the Mackenzie drainage basin to the Arctic Ocean. *Environmental Research Letters*, *11*(5), 054015. https://doi.org/10.1088/1748-9326/11/5/054015

Tarnocai, C., Swanson, D., Kimble, J., & Broll, G. (2007). *Northern circumpolar soil carbon database, digital database*. Ottawa, ON: Research Branch, Agriculture and Agri-Food Canada.

Townsend-Small, A., McClelland, J. W., Holmes, R. M., & Peterson, B. J. (2011). Seasonal and hydrologic drivers of dissolved organic matter and nutrients in the upper Kuparuk River, Alaskan Arctic. *Biogeochemistry*, *103*(1–3), 109–124. https://doi.org/10.1007/s10533-010-9451-4

Tremblay, J.-É., Anderson, L. G., Matrai, P., Coupel, P., Bélanger, S., Michel, C., & Reigstad, M. (2015). Global and regional drivers of nutrient supply, primary production and CO_2 drawdown in the changing Arctic Ocean. *Progress in Oceanography*, *139*, 171–196. https://doi.org/10.1016/j.pocean.2015.08.009

Venables, W. N., & Ripley, B. D. (2002). *Modern Applied Statistics with S* (4th ed.). New York, NY: Springer.

Wauthy, M., Rautio, M., Christoffersen, K. S., Forsström, L., Laurion, I., Mariash, H. L., et al. (2018). Increasing dominance of terrigenous organic matter in circumpolar freshwaters due to permafrost thaw. *Limnology and Oceanography Letters*, *3*(3), 186–198. https://doi.org/10.1002/lol2.10063

Wheeler, J. O., Hoffman, P. F., Card, K. D., Davidson, A., Sanford, B. V., Okulitch, A. V., & Roest, W. R. (1996). *Geological map of Canada (Map D1860A)*. Ottawa, ON: Natural Resources Canada.

White, D., Hinzman, L., Alessa, L., Cassano, J., Chambers, M., Falkner, K., et al. (2007). The arctic freshwater system: Changes and impacts. *Journal of Geophysical Research*, *112*, G04S54. https://doi.org/10.1029/2006JG000353

Yang, D., Shi, X., & Marsh, P. (2015). Variability and extreme of Mackenzie River daily discharge during 1973–2011. *Quaternary International*, *380-381*, 159–168. https://doi.org/10.1016/j.quaint.2014.09.023

Yang, D., Zhao, Y., Armstrong, R., Robinson, D., & Brodzik, M. J. (2007). Streamflow response to seasonal snow cover mass changes over large Siberian watersheds. *Journal of Geophysical Research*, *112*, F02S22. https://doi.org/10.1029/2006JF000518